Nonlocal chiral quark models with wavefunction renormalization: sigma properties and $\pi - \pi$ scattering parameters

S. Noguera[a*] and N.N. Scoccola[b,c,d†]
[a] *Departamento de Fisica Teorica and Instituto de Fisica Corpuscular, Universidad de Valencia-CSIC, E-46100 Burjassot (Valencia), Spain.*
[b] *CONICET, Rivadavia 1917, 1033 Buenos Aires, Argentina*
[c] *Physics Department, Comisión Nacional de Energía Atómica, Av. Libertador 8250, 1429 Buenos Aires, Argentina and*
[d] *Universidad Favaloro, Solís 453, 1078 Buenos Aires, Argentina*

We analyze the sigma meson mass and width together with the pion-pion scattering parameters in the context of non-local chiral quark models with wave-function renormalization (WFR). We consider both non-local interactions based on the frequently used exponential form factor, and on fits to the quark mass and renormalization functions obtained in lattice calculations. In the case of the sigma properties we obtain results which are less dependent on the parameterization than in the standard local NJL model, and which are in reasonable agreement with the recently reported empirical values. We also show that the inclusion of the WFR tend to improve the description of the π-π scattering parameters, with the lattice inspired parameterization providing the best overall results. Finally, we analyze the connection of the non-local quark models discussed here with Chiral Perturbation Theory, and present the model predictions for the low energy constants relevant for π-π scattering to $O(4)$ in the chiral expansion.

I. INTRODUCTION

Although much effort has been made in trying to predict low energy hadron observables directly from QCD, one is still far from reaching this goal due to the extremely complex non-perturbative behavior of the theory in that regime. In such a situation it proves convenient to turn to the study of effective models. For two light flavors it is believed that QCD supports an approximate SU(2) chiral symmetry which is dynamically broken at low energies, and pions play the role of the corresponding Goldstone bosons. A simple scheme including these properties is the well known Nambu−Jona-Lasinio (NJL) model [1], proposed more than four decades ago. The NJL model has been widely used as an schematic effective theory for QCD [2, 3, 4], allowing e.g. the description of light mesons as fermion-antifermion composite states. In the NJL model quarks interact through a local, chiral invariant four-fermion coupling. Because of the local nature of this interaction, the corresponding Schwinger-Dyson and Bethe-Salpeter equations become relatively simplified. However, the main drawbacks of the model are direct consequences of this locality: loop integrals are divergent (and therefore have to be regulated somehow), and the model is nonconfining. As a way to improve upon the NJL model, extensions which include nonlocal interactions have been proposed (see Ref. [5] and references therein). In fact, nonlocality arises naturally in quantum field theory and, particularly, in several well established approaches to low energy quark dynamics, as e.g. the instanton liquid model [6] and the Schwinger-Dyson resummation techniques [7]. Lattice QCD calculations [8, 9, 10] also indicate that quark interactions should act over a certain range in the momentum space. Moreover, it has been argued that nonlocal extensions of the NJL model do not show some of the above mentioned inconveniences of the local theory. Indeed, nonlocal interactions regularize the model in such a way that anomalies are preserved [11] and charges are properly quantized, the effective interaction is finite to all orders in the loop expansion and therefore there is not need to introduce extra cutoffs [12], soft regulators such as Gaussian functions lead to small next-to-leading order corrections [13], etc.

In the present work we will reconsider non-local models adopting as the basic ingredient a reliable description of the quark propagator as given from fundamental studies, such as lattice QCD. In this sense, it should be noticed that, except for Ref.[14, 15], most of the calculation performed so far using non-local chiral quark models have neglected the wave function renormalization in the propagator (See e.g. Refs. [16, 17, 18, 19, 20]). Recent lattice QCD calculations suggest, however, that such renomalization can be of the order of 30 % (or even more) at zero momentum[8, 9, 10]. Moreover, these calculations also show that the quark masses tend to their asymptotic values in a rather soft way. Thus, it is of importance to perform a detailed study on the incorporation of these features in this type of models,

*Electronic address: Santiago.Noguera@uv.es
†Electronic address: scoccola@tandar.cnea.gov.ar

and analyze their role in the prediction for different hadronic observables. The lagrangian we will use is the minimal extension which allows to incorporate the full momentum dependence of the quark propagator, through its mass and wave function renormalization. Using this lagrangian we explore which are the implications for some pion and sigma meson properties originated by changes in the quark propagator. In particular, we present here results for the sigma meson mass and width, and for the pion-pion scattering parameters. Studying these scattering parameters close to the chiral limit we are also able to obtain predictions for some of the low energy constants of the Chiral Perturbation Theory (χPT) Lagrangian [21].

The present article is organized as follows. In Sec. II we present the model lagrangian and the formalism necessary to derive some selected pion and sigma meson properties. In Sec. III we discuss different ways to obtain the model parameters and compare the resulting quark propagators with available lattice data. In Sec. IV we present and discuss the predictions of the model for the selected parametrizations, paying special attention to the role played by the incorporation of the wavefunction renormalization and by the difference in the quark interaction momentum dependence. In Sec. V we analyze the connection of the non-local quark models described here with χPT, and present the predictions for the corresponding low energy constants relevant for π-π scattering to $O(4)$ in the chiral expansion. Finally, in Sec. VI our main conclusions are summarized.

II. THE MODEL

A. Effective action

Let us begin by stating the Euclidean action for the nonlocal chiral quark model in the case of two light flavors,

$$S_E = \int d^4x \, \left\{ \bar{\psi}(x) \left(-i\partial\!\!\!/ + m_c\right) \psi(x) - \frac{G_S}{2} \Big[j_a(x) j_a(x) - j_P(x) j_P(x) \Big] \right\} \, . \tag{1}$$

Here m_c is the current quark mass, which is assumed to be equal for u and d quarks. The nonlocal currents $j_a(x), j_P(x)$ are given by

$$\begin{aligned} j_a(x) &= \int d^4z \; g(z) \; \bar{\psi}\left(x + \frac{z}{2}\right) \; \Gamma_a \; \psi\left(x - \frac{z}{2}\right) \; . \\ j_P(x) &= \int d^4z \; f(z) \; \bar{\psi}\left(x + \frac{z}{2}\right) \; \frac{i \overleftrightarrow{\partial\!\!\!/}}{2 \; \varkappa_p} \; \psi\left(x - \frac{z}{2}\right) \end{aligned} \tag{2}$$

Here, $\Gamma_a = (\mathbf{1}, i\gamma_5\vec{\tau})$ and $u(x') \overleftrightarrow{\partial} v(x) = u(x')\partial_x v(x) - \partial_{x'} u(x') v(x)$. The functions $g(z)$ and $f(z)$ in Eq.(2), are nonlocal covariant form factors characterizing the corresponding interactions. The four standard quark currents, $j_a(x)$, require the same $g(z)$ form factor to guarantee chiral invariance. The new term, $j_P(x)j_P(x)$, is self-invariant under chiral transformations. The scalar-isoscalar component of the $j_a(x)$ current will generate the momentum dependent quark mass in the quark propagator, while the "momentum" current, $j_P(x)$, will be responsible for a momentum dependent wave function renormalization of this propagator. For convenience, we take the same coupling parameter, G_S, for the standard chiral quark interaction and for the new $j_P(x)j_P(x)$ term. Note, however, that the relative strength between both interaction terms will be controlled by the mass parameter $\varkappa_p$ introduced in Eq.(2). We have choosen the relative sign between these terms in order to have a real value for $\varkappa_p$ for the case in which the wave function renormalization $Z(p)$ (explicitly defined in Eq.(10 below) is less than 1. In what follows it is convenient to Fourier transform $g(z)$ and $f(z)$ into momentum space. Note that Lorentz invariance implies that the Fourier transforms $g(p)$ and $f(p)$ can only be functions of p^2.

In order to deal with meson degrees of freedom, one can perform a standard bosonization of the theory. This is done by considering the corresponding partition function $\mathcal{Z} = \int \mathcal{D}\bar{\psi}\,\mathcal{D}\psi \, \exp[-S_E]$, and introducing auxiliary fields $\sigma_1(x), \sigma_2(x), \vec{\pi}(x))$, where $\sigma_{1,2}(x)$ and $\vec{\pi}(x)$ are scalar and pseudoscalar mesons, respectively. Integrating out the quark fields we get

$$\mathcal{Z} = \int \mathcal{D}\sigma_1 \, \mathcal{D}\sigma_2 \; \mathcal{D}\vec{\pi} \; \exp[-S_E^{\rm bos}] \; , \tag{3}$$

where

$$S_E^{\rm bos} = -\ln \det A + \frac{1}{2G_S} \int \frac{d^4p}{(2\pi)^4} \; \left[\sigma_1(p) \; \sigma_1(-p) + \vec{\pi}(p) \cdot \vec{\pi}(-p) + \sigma_2(p) \; \sigma_2(-p)\right] . \tag{4}$$

The operator A reads, in momentum space,

$$A(p,p')=(-\not{p}+m_c)\,(2\pi)^4\,\delta^{(4)}(p-p')+g\left(\frac{p+p'}{2}\right)\,[\sigma_1(p'-p)+i\gamma_5\vec{\tau}\cdot\vec{\pi}(p'-p)] \\ +\;f\left(\frac{p+p'}{2}\right)\,\frac{\not{p}+\not{p}'}{2\,\varkappa_p}\,\sigma_2(p'-p), \tag{5}$$

At this stage we assume that the $\sigma_{1,2}$ fields have nontrivial translational invariant mean field values $\bar{\sigma}_{1,2}$, while the mean field values of the pseudoscalar fields π_i are zero. Thus we write

$$\sigma_1(x) = \bar{\sigma}_1 + \delta\sigma_1(x) \tag{6}$$
$$\sigma_2(x) = \varkappa_p\;\bar{\sigma}_2 + \delta\sigma_2(x) \tag{7}$$
$$\vec{\pi}(x) = \delta\vec{\pi}(x) \tag{8}$$

Replacing in the bosonized effective action, and expanding in powers of the meson fluctuations, we get

$$S_E^{\rm bos} \;=\; S_E^{\rm MFA} + S_E^{\rm quad} + \;...$$

Here the mean field action per unit volume reads

$$\frac{S_E^{\rm MFA}}{V^{(4)}} = -2N_c\int\frac{d^4p}{(2\pi)^4}\;{\rm tr}\ln\left[\mathcal{D}_0^{-1}(p)\right] + \frac{\bar{\sigma}_1^2}{2G_S} + \frac{\varkappa_p^2\;\bar{\sigma}_2^2}{2G_S}\;, \tag{9}$$

where the quark propagator in the mean field approximation $\mathcal{D}_0(p)$ is given by

$$\mathcal{D}_0(p) = \frac{Z(p)}{-\not{p}+M(p)} \tag{10}$$

with

$$Z(p) = (1-\bar{\sigma}_2\;f(p))^{-1} \\ M(p) = Z(p)\,(m_c+\bar{\sigma}_1\;g(p)) \tag{11}$$

The quadratic terms can be written as

$$S_E^{\rm quad} = \frac{1}{2}\int\frac{d^4p}{(2\pi)^4}\left[G_\sigma(p^2)\;\delta\sigma(p)\;\delta\sigma(-p)+G_{\sigma'}(p^2)\;\delta\sigma'(p)\;\delta\sigma'(-p)+\;G_\pi(p^2)\;\delta\vec{\pi}(p)\cdot\delta\vec{\pi}(-p)\right]\;, \tag{12}$$

where the σ and σ' fields are related to σ_1 and σ_2 by

$$\delta\sigma = \cos\theta\;\;\delta\sigma_1 - \sin\theta\;\;\delta\sigma_2 \tag{13}$$
$$\delta\sigma' = \sin\theta\;\;\delta\sigma_1 + \cos\theta\;\;\delta\sigma_2\;, \tag{14}$$

and the mixing angle θ is defined in such a way that there is no $\sigma-\sigma'$ mixing at the level of the quadratic action. The function $G_\pi(p^2)$ introduced in Eq. (12) is given by

$$G_\pi(p^2) = \frac{1}{G_S} - \,8\,N_c\int\frac{d^4q}{(2\pi)^4}\;g^2(q)\frac{Z(q^+)Z(q^-)}{D(q^+)D(q^-)}\left[q^+\cdot q^- + M(q^+)M(q^-)\right] \tag{15}$$

with $q^\pm = q\pm p/2$ and $D(q)=q^2+M^2(q)$, while for the $\sigma-\sigma'$ system we have

$$G_{\begin{pmatrix}\sigma\\ \sigma'\end{pmatrix}}(p^2) = \frac{G_{\sigma_1\sigma_1}(p^2)+G_{\sigma_2\sigma_2}(p^2)}{2} \mp \sqrt{[G_{\sigma_1\sigma_2}(p^2)]^2+\left[\frac{G_{\sigma_1\sigma_1}(p^2)-G_{\sigma_2\sigma_2}(p^2)}{2}\right]^2} \tag{16}$$

where

$$G_{\sigma_1\sigma_1}(p^2) = \frac{1}{G_S} - \,8\,N_c\int\frac{d^4q}{(2\pi)^4}\;g^2(q)\frac{Z(q^+)Z(q^-)}{D(q^+)D(q^-)}\left[q^+\cdot q^- - M(q^+)M(q^-)\right] \\ G_{\sigma_2\sigma_2}(p^2) = \frac{1}{G_S} + \frac{8\,N_c}{\varkappa_p^2}\;\int\frac{d^4q}{(2\pi)^4}\;q^2f^2(q)\frac{Z(q^+)Z(q^-)}{D(q^+)D(q^-)}\left[(q^+\cdot q^-) - M(q^+)M(q^-) + \frac{(q^+)^2(q^-)^2-(q^+\cdot q^-)^2}{2q^2}\right] \\ G_{\sigma_1\sigma_2}(p^2) = -\frac{8\,N_c}{\varkappa_p}\;\int\frac{d^4q}{(2\pi)^4}\;g(q)f(q)\frac{Z(q^+)Z(q^-)}{D(q^+)D(q^-)}\;q\cdot\left[q^-M(q^+)+q^+M(q^-)\right] \tag{17}$$

B. Mean field approximation and chiral condensates

In order to find the mean field values $\bar{\sigma}_{1,2}$, one has to minimize the action $S_E^{\rm MFA}$. A straightforward exercise leads to the coupled gap equations

$$\bar{\sigma}_1 - 8N_c\ G_S \int \frac{d^4p}{(2\pi)^4}\ g(p)\ \frac{Z(p)M(p)}{D(p)} = 0$$
$$\bar{\sigma}_2 + 8N_c\ G_S \int \frac{d^4p}{(2\pi)^4}\ \frac{p^2}{\varkappa_p^2}\ f(p)\ \frac{Z(p)}{D(p)} = 0. \tag{18}$$

Now the chiral condensates are given by the vacuum expectation values $\langle\bar{q}q\rangle = \langle\bar{u}u\rangle = \langle\bar{d}d\rangle$. They can be easily obtained by performing the variation of $\mathcal{Z}^{\rm MFA} = \exp[-S_E^{MFA}]$ with respect to the corresponding current quark masses. This expression turns out to be divergent. Thus, as customary, we regularize it by subtracting its value for non-interacting quarks. We obtain

$$\langle\,\bar{q}\,q\,\rangle = -\,4N_c \int \frac{d^4p}{(2\pi)^4}\ \left(\frac{Z(p)M(p)}{D(p)} - \frac{m_c}{p^2+m_c^2}\right).$$

C. Meson masses and quark-meson coupling constants

The meson masses can be obtained by solving the equation

$$G_M(-m_M^2) = 0\ . \tag{19}$$

In the case of the $\sigma - \sigma'$ system the mixing angles is given by $\theta(-m^2_{\sigma,\sigma'})$, where

$$\tan 2\ \theta(p^2) = \frac{2G_{\sigma_1\sigma_2}(p^2)}{G_{\sigma_2\sigma_2}(p^2) - G_{\sigma_1\sigma_1}(p^2)} \tag{20}$$

Finally, the on-shell meson-quark coupling constants $g_{Mq\bar{q}}$ are given by

$$g_{Mq\bar{q}}^{-2} \equiv G_{Mq\bar{q}}^{-2}(-m_M^2)\ =\ \left.\frac{dG_M(p)}{dp^2}\right|_{p^2=-m_M^2}\ . \tag{21}$$

Note that due to the mixing, in the scalar meson channel the corresponding vertex has two components. Thus for $\sigma q\bar{q}$ vertex we have

$$V_{\sigma q\bar{q}} = g^0_{\sigma q\bar{q}}\ \mathbf{1} + g^1_{\sigma q\bar{q}}\frac{\not{p}+\not{p}'}{2\varkappa_p} \tag{22}$$

where

$$g^{(0)}_{\sigma q\bar{q}} = g_{\sigma q\bar{q}}\ \cos\theta \qquad ; \qquad g^{(1)}_{\sigma q\bar{q}} = g_{\sigma q\bar{q}}\ \sin\theta \tag{23}$$

D. Pion weak decay constant

By definition the pion weak decay constant f_π is given by the matrix element of the axial current $A^a_\mu(x)$ between the vacuum and the renormalized one-pion state at the pion pole:

$$\langle 0|A^a_\mu(0)|\tilde{\pi}^b(p)\rangle = i\ \delta^{ab}\ p_\mu\ f_\pi\ . \tag{24}$$

In order to obtain an explicit expression for the axial current, we have to "gauge" the effective action S_E by introducing a set of axial gauge fields $\mathcal{A}^a_\mu(x)$. For a local theory this "gauging" procedure is usually done by performing the replacement

$$\partial_\mu \to \partial_\mu + \frac{i}{2}\ \gamma_5\ \vec{\tau}\cdot\vec{\mathcal{A}}_\mu(x)\ . \tag{25}$$

In the present case —owing to the nonlocality of the involved fields— one has to perform additional replacements in the interaction terms. Namely,

$$\begin{aligned}\psi(x-z/2) \;&\rightarrow\; W_A\,(x,x-z/2)\;\psi(x-z/2)\\ \psi^\dagger(x+z/2) \;&\rightarrow\; \psi^\dagger(x+z/2)\;W_A\,(x+z/2,x)\end{aligned} \tag{26}$$

Here x and z are the variables appearing in the definitions of the nonlocal currents (see Eq.(2)), and the function $W_A(x,y)$ is defined by

$$W_A(x,y) \;=\; \mathrm{P}\;\exp\left[\frac{i}{2}\int_x^y ds_\mu\;\gamma_5\;\vec{\tau}\cdot\vec{\mathcal{A}}_\mu(s)\right]\;, \tag{27}$$

where s runs over an arbitrary path connecting x with y.

Once the gauged effective action is built, it is easy to get the axial current as the derivative of this action with respect to $\mathcal{A}^a_\mu(x)$, evaluated at $\vec{\mathcal{A}}_\mu(x)=0$. Performing the derivative of the resulting expressions with respect to the renormalized meson fields, we can finally identify the corresponding meson weak decay constants. After a rather lengthy calculation we obtain

$$f_\pi = \frac{m_c\;g_{\pi q\bar{q}}}{m_\pi^2}\;F_0(-m_\pi^2)\;. \tag{28}$$

with

$$F_0(p^2) = 8\,N_c\int\frac{d^4q}{(2\pi)^4}\;g(q)\;\frac{Z(q^+)Z(q^-)}{D(q^+)D(q^-)}\;\left[q^+\cdot q^- + M(q^+)M(q^-)\right] \tag{29}$$

It is important to notice that the integration over the path variable s appearing in this calculation turns out to be trivial and, thus, the result path-independent. In the chiral limit the expression Eq.(28) has a rather simple form [14] given by

$$f_\pi = \frac{M\,(0)}{g_{\pi qq}Z\,(0)} \quad\;, \tag{30}$$

which connects with the Goldberger-Treiman relation.

E. The decay width of the Sigma meson

To obtain the decay amplitude of the σ meson into two pion we need to calculate

$$\frac{\delta S_E^{\mathrm{bos}}}{\delta\sigma(q)\delta\pi^a(q_1)\delta\pi^b(q_2)} = (2\pi)^4\;\delta^4(q+q_1+q_2)\;\delta_{ab}\;G_{\sigma\pi\pi}(q^2,q_1^2,q_2^2) \tag{31}$$

where the meson fields are assumed to be already renormalized. In terms of the unrenormalized fields and taking into account the $\sigma_1-\sigma_2$ mixing we have

$$G_{\sigma\pi\pi}(q^2,q_1^2,q_2^2) = G_{\sigma q\bar{q}}(q^2)\;G_{\pi q\bar{q}}(q_1^2)\;G_{\pi q\bar{q}}(q_2^2)\;\tilde{G}_{\sigma\pi\pi}(q^2,q_1^2,q_2^2) \tag{32}$$

where

$$\tilde{G}_{\sigma\pi\pi}(q^2,q_1^2,q_2^2) = G_{\sigma_1\pi\pi}(q^2,q_1^2,q_2^2)\;\cos\theta(q^2) - G_{\sigma_2\pi\pi}(q^2,q_1^2,q_2^2)\;\sin\theta(q^2) \tag{33}$$

and the expressions of the unrenormalized σ_1 and σ_2 coupling constants to two π can be obtained by expanding Γ to third order in the fluctuations. We get

$$\begin{aligned}G_{\sigma_1\pi\pi}(q^2,q_1^2,q_2^2) = -16N_c\int\frac{d^4k}{(2\pi)^4}\;\; g\left(\frac{k_1+k_2}{2}\right)g\left(\frac{k+k_1}{2}\right)g\left(\frac{k+k_2}{2}\right)\frac{Z(k)Z(k_1)Z(k_2)}{D(k)D(k_1)D(k_2)}\times\\ \times\left[M(k)\;k_1\cdot k_2 - M(k_1)\;k\cdot k_2 - M(k_2)\;k\cdot k_1 - M(k)\;M(k_1)\;M(k_2)\right]\end{aligned} \tag{34}$$

$$\begin{aligned}G_{\sigma_2\pi\pi}(q^2,q_1^2,q_2^2) = -\frac{8N_c}{\varkappa_p}\;\int\frac{d^4k}{(2\pi)^4}\;\; f\left(\frac{k_1+k_2}{2}\right)g\left(\frac{k+k_1}{2}\right)g\left(\frac{k+k_2}{2}\right)\frac{Z(k)Z(k_1)Z(k_2)}{D(k)D(k_1)D(k_2)}\times\\ \times\left[k_2^2\;k\cdot k_1 + k_1^2\;k\cdot k_2 + (k_1+k_2)\cdot[M(k_1)\;M(k)\;k_2 - M(k_2)\;M(k_1)\;k + M(k_2)\;M(k)\;k_1]\right]\end{aligned} \tag{35}$$

where $k_1 = k + q_1$ and $k_2 = k - q_2$ and $q^2 = (q_1 + q_2)^2$. Similarly for σ' we have

$$G_{\sigma'\pi\pi}(q^2, q_1^2, q_2^2) = G_{\sigma' q\bar{q}}(q^2)\ G_{\pi q\bar{q}}(q_1^2)\ G_{\pi q\bar{q}}(q_2^2)\ \tilde{G}_{\sigma'\pi\pi}(q^2, q_1^2, q_2^2) \tag{36}$$

where

$$\tilde{G}_{\sigma'\pi\pi}(q^2, q_1^2, q_2^2) = G_{\sigma_1\pi\pi}(q^2, q_1^2, q_2^2)\ \sin\theta(q^2) + G_{\sigma_2\pi\pi}(q^2, q_1^2, q_2^2)\ \cos\theta(q^2) \tag{37}$$

In terms of $g_{M\pi\pi} = G_{M\pi\pi}(m_M^2, m_\pi^2, m_\pi^2)$ the $M = \sigma, \sigma'$ width reads

$$\Gamma_{M\to\pi\pi} = \frac{3}{2}\frac{g_{M\pi\pi}^2}{16\pi m_M}\sqrt{1 - \frac{4m_\pi^2}{m_M^2}} \tag{38}$$

F. π-π scattering

In general, the total amplitude for the π-π scattering process can be expressed as

$$\mathcal{A}\left(\pi^\alpha(q_1) + \pi^\beta(q_2) \to \pi^\gamma(q_3) + \pi^\delta(q_4)\right) = \delta_{\alpha\beta}\delta_{\gamma\delta}A(s,t,u) + \delta_{\alpha\gamma}\delta_{\beta\delta}A(t,s,u) + \delta_{\alpha\delta}\delta_{\beta\gamma}A(u,t,s) \tag{39}$$

where

$$s = (q_1 + q_2)^2 \qquad ; \qquad t = (q_1 - q_3)^2 \qquad ; \qquad u = (q_1 - q_4)^2 \tag{40}$$

Within the present model, this amplitude gets two contributions. One corresponds to the box diagram and the other to the scalar meson pole diagram. Thus,

$$A(s,t,u) = A_{box}(s,t,u) - g_{\pi q\bar{q}}^4 \sum_{M=\sigma,\sigma'} \tilde{G}_{M\pi\pi}^2(s, m_\pi^2, m_\pi^2)\ G_M^{-1}(s) \tag{41}$$

where

$$A_{box}(s,t,u) = g_{\pi q\bar{q}}^4\ \left[J(s,t,u) + J(s,u,t) - J(u,t,s)\right] \tag{42}$$

and

$$J\left(s,t,u\right) = \frac{1}{2}\left[J_{box}\left(q_1,q_2,q_3\right) + J_{box}\left(q_1,-q_3,-q_2\right)\right] \tag{43}$$

with

$$\begin{aligned} J_{box}\left(q_1,q_2,q_3\right) = 16N_c \int \frac{d^4k}{2\pi}\ g\left(\frac{k+k_1}{2}\right)\ g\left(\frac{k+k_2}{2}\right)\ g\left(\frac{k_1+k_{13}}{2}\right)\ g\left(\frac{k_2+k_{13}}{2}\right) \frac{Z(k_1)Z(k)Z(k_2)Z(k_{13})}{D(k_1)D(k)D(k_2)D(k_{13})} \times \\ \Big\{ \left[k_1\cdot k + M(k_1)M(k)\right]\left[k_2\cdot k_{13} + M(k_1)M(k_{13})\right] - \left[k_1\cdot k_2 + M(k_1)M(k_2)\right]\left[k\cdot k_{13} + M(k)M(k_{13})\right] \\ + \left[k_1\cdot k_{13} + M(k_1)M(k_{13})\right]\left[k\cdot k_2 + M(k)M(k_2)\right] \Big\} \end{aligned} \tag{44}$$

where $k_1 = k + q_1$, $k_2 = k - q_2$, $k_{13} = k + q_1 - q_3$.

It is customary to define the scattering amplitudes of defined isospin

$$\begin{aligned} T^0 &= 3A(s,t,u) + A(t,s,u) + A(u,t,s) \\ T^1 &= A(t,s,u) - A(u,t,s) \\ T^2 &= A(t,s,u) + A(u,t,s) \end{aligned} \tag{45}$$

In terms of these amplitudes the scattering lengths a_ℓ^I and slope parameters b_ℓ^I are defined by the partial wave expansion at low q^2

$$\frac{1}{64\pi m_\pi}\int_{-1}^{1} dx\ P_\ell(x)\ T^I(s,t,u) = q^{2\ell}\left(a_\ell^I + b_\ell^I\ q^2 + ...\right) \tag{46}$$

where $P_\ell(x)$ is the Lagrange polynomial of order l.

III. DETERMINATION OF THE MODEL PARAMETERS

In this section we present in some detail the procedure used to determine the model parameters as well as the form factors $g(q)$ and $f(q)$ which characterize the non-local interactions.

In our first model (scenario S1) we use exponential functions to model the non-local interactions. These are well behaved functions which have been often used in the literature (see e.g. [16, 17, 18, 19]) to define $g(q)$. Here, we also use such form for $f(q)$. Thus, for S1 we have

$$g(p) = \exp(-p^2/\Lambda_0^2) \qquad ; \qquad f(p) = \exp(-p^2/\Lambda_1^2) \tag{47}$$

Note that the range (in momentum space) of the nonlocality in each channel is determined for the parameters Λ_0 and Λ_1, respectively. From Eq. (11) we obtain

$$\begin{aligned} M\left(p\right) &= Z\left(p\right)\ \left[m_c + \bar{\sigma}_1\ \exp(-p^2/\Lambda_0^2)\right] \\ Z\left(p\right) &= \left[1 - \bar{\sigma}_2\ \exp(-p^2/\Lambda_1^2)\right]^{-1} \end{aligned} \tag{48}$$

We fix the values of m_c and $< q\bar{q} >^{1/3}$ to reasonable values $m_c = 5.7$ MeV and $< q\bar{q} >^{1/3} = -240$ MeV determining the rest of the parameters so as to reproduce the empirical values $f_\pi = 92.4$ MeV and $m_\pi = 139$ MeV, and $Z(0) = 0.7$ which is within the range of values suggested by recent lattice calculations[8, 10].

For the second parametrization we follow Ref.[14], where a parametrization based on a fit to the mass and renormalization functions obtained in a Landau gauge lattice calculation was used. Such parametrization is

$$\begin{aligned} M(p) &= m_c + \alpha_m\ f_m(p)\ \ , \\ Z(p) &= 1 + \alpha_z\ f_z(p) \qquad , \end{aligned} \tag{49}$$

with

$$f_m(p) = \left[1 + \left(p^2/\Lambda_0^2\right)^{3/2}\right]^{-1} \qquad ; \qquad f_z(p) = \left[1 + \left(p^2/\Lambda_1^2\right)\right]^{-5/2} \quad , \tag{50}$$

where the analytical form of $f_m\left(p\right)$ has been proposed in Ref.[9]. The analytical form of $f_z\left(p\right)$ is chosen in order to guarantee the convergence of the integrals. Some alternative parametrization of this type suggested from vector meson dominance of the pion form factor can be found in Ref.[22]. In terms of the functions $f_m(p)$ and $f_z(p)$, and the constants m_c, α_m, α_z the form factors $g(q)$ and $f(q)$ are given by

$$\begin{aligned} g(p) &= \frac{1+\alpha_z}{1+\alpha_z f_z(p)} \frac{\alpha_m f_m(p) - m_c \alpha_z f_z(p)}{\alpha_m - m_c \alpha_z} \quad , \\ f(p) &= \frac{1+\alpha_z}{1+\alpha_z f_z(p)}\ f_z(p) \quad . \end{aligned} \tag{51}$$

and the mean field values are

$$\begin{aligned} \bar{\sigma}_1 &= \frac{\alpha_m - m_c \alpha_z}{1+\alpha_z} \\ \bar{\sigma}_2 &= \frac{\alpha_z}{1+\alpha_z} \end{aligned} \tag{52}$$

The parameters for this second model (scenario S2) are determine as follows. As before we take $Z(0) = 0.7$ and fix Λ_0 and Λ_1 in such a way that the functions $f_m\left(p\right)$ and $Z\left(p\right)$ agree reasonable well with lattice results of Ref.[8]. Next we fix m_c and α_m in order to reproduce the physical values of m_π and f_π. The resulting parameters are $m_c = 2.37$ MeV, $\alpha_m = 309$ MeV, and with $\Lambda_0 = 850$ MeV and $\Lambda_1 = 1400$ MeV.

Finally, in order to compare with previous studies where the wavefunction renormalization of the quark propagator has been ignored we consider a third model (scenario S3). In such scenario we take $Z(p) = 1$ and exponential parametrization for $g(p)$. Such model corresponds to the "Model II" discussed in Ref.[18], from where we take the parameters corresponding to $< q\bar{q} >^{1/3} = -240$ MeV.

The values of the model parameters for each of the chosen scenarios are summarized in Table I. In Fig.1 we compare the quark mass function $f_m(p)$ and renormalization function $Z(p)$ as obtained from our three scenarios with data extracted from the lattice results of Ref.[8]. The main reason for comparing $f_m(p)$ (instead of $M\left(p\right)$) is that analyzing lattice data from different groups using Landau gauge fixing[8, 10], and also results for $M\left(p\right)$ obtained by each group using different inputs, we observed that the resulting functions $f_m(p)$ are very similar in spite of the

differently looking $M(p)$. On the other hand, the renomalization functions $Z\,(p)$ are much less sensitive to the choice of lattice parameters, and in fact the two lattice groups [8, 10] provide similar results. We observe that the functions $f_m\,(p)$ and $Z\,(p)$ for scenario S1, based on exponential functions, decrease faster than the lattice data. For scenario S2, however, they go to zero as $(p^2)^{-3/2}$ and $(p^2)^{-5/2}$, respectively, following the lattice data in a closer manner. Finally, in the case of S3 the exponential decrease of $f_m(p)$ is even faster than that of S_1.

IV. NUMERICAL RESULTS

In this section we present and discuss our numerical results. In Table I we give the results for the mean-field properties, together with the pion and sigma masses and decay parameters. As it can be seen in this table, while for the exponential parameterizations (i.e. S1 and S3) the empirical values of f_π and m_π are consistent with a quark condensate which lies within the range of the usually quoted phenomenological values $-\langle\bar{q}q\rangle^{1/3} \simeq 200$ - 260 MeV [23, 24] the scenario S2 leads to a value of the chiral condensate somewhat above such range. On the other hand, the corresponding current quark mass is quite smaller than those obtained for the scenarios S1 and S3. This issue deserves some comment. The chiral condensate, as well as the current quark masses, are scale dependent objects. In particular, the phenomenological values quoted above for the condensate correspond to a choice of the renormalization scale $\mu = 1$ GeV. In the parametrization S2 some parameters have been determined so as to obtain a good approximation to the lattice mass renormalization function $Z(p)$, a quantity which also depends on the renormalization point. In particular, we use the function $Z(p)$ obtained in Ref.[8] where the renormalization scale has been chosen to be $\mu = 3$ GeV. One might wonder whether the fact that this renormalization point differs from the one usually used to quote the values of the condensate can account for the fact that the S2 prediction is outside the empirical range. If one assumes that this difference is also responsible for the rather low value of m_c this can be investigated in the following way. To leading order in the chiral expansion the current quark mass and the condensate are related by the Gell-Mann-Oakes-Renner (GMOR) relation

$$f_\pi^2\, m_\pi^2 = 2 < \bar{q}q > \hat{m} \tag{53}$$

where $\hat{m} = (m_u + m_d)/2$. The validity of GMOR to that order is well justified by the low energy behavior of the $\pi\pi$ scattering amplitudes [25]. Using that, according to Ref.[26], $\hat{m}$ runs from 5.5 MeV at the scale $\mu = 1$ GeV to 4.1 MeV at $\mu = 2$ GeV we expect that a typical value of $\langle\bar{q}q\rangle^{1/3} = -240$ MeV at $\mu = 1$ GeV will run to $\langle\bar{q}q\rangle^{1/3} = -270$ MeV at $\mu = 2$ GeV [27]. Lattice calculations provide an independent determination of quark masses and $\bar{q}q$ condensate [28, 29, 30]:

$$m_{ud}^{\overline{MS}}\,(2\ GeV) = 4.3 \pm 0.4_{stat}\, {}^{+1.1}_{-0.4}{}_{sys}\ MeV \tag{54}$$

$$\langle\bar{q}q\rangle\,(2\ GeV) = -\,(265 \pm 5_{stat} \pm 22_{sys} MeV)^3 \tag{55}$$

which confirms the $\mu = 2$ GeV values given above. Note that since these two lattice calculations are not connected, the quoted values imply a verification of the GMOR relation. Since the GMOR relation is well satisfied by our lagrangian model [14], and in all our scenarios f_π and m_π are fitted to their empirical values, it is clear that the quality of the description of the quark condensate and the current quark mass are closely related. Thus, a further running up to $\mu = 3\ GeV$ implies that the current quark mass must be scaled by a factor of the $\hat{m}(2\text{ GeV})/\hat{m}(3\text{ GeV}) = 1.11$. This value is rather different from the factor 1.81 obtained from the ratio between the lattice result at $\mu = 2$ GeV and the value of m_c for the scenario S2 given in Table I. This clearly indicates that possible ambiguities related to the choice of renormalization point cannot fully account for the rather high value of the condensate for the scenario S2. In fact, using the above mentioned factors to reescale the value $-\langle\bar{q}q\rangle^{1/3} \simeq 326$ MeV quoted in Table I down to $\mu = 1\ GeV$ we get $-\langle\bar{q}q\rangle^{1/3} \simeq 284$ MeV which is about 10% above the empirical upper limit. A possible way to reduce the value of the quark condensate in S2 is to reduce the parameter Λ_0. For $\Lambda_0 \sim 600$ MeV we can obtain values for the quark condensate and quark masses which are within the phenomenological bounds.

The mass and width of the sigma meson display some dependence on the parametrization. However, such dependence is smaller than the one found in the local NJL model[31]. The obtained values for the masses are somewhat larger than the recently extracted empirical values $478^{+24}_{-23} \pm 17 MeV$ [32] and $390^{+60}_{-36} MeV$ [33] while the widths are compatible with the experimentally reported values $324^{+42}_{-40} \pm 21 MeV$ [32] and $282^{+77}_{-50} MeV$ [33].

The situation concerning the σ' meson deserves some comment. In general, for the non-local models under consideration the quark propagators develop a series of poles in the complex plane. In Euclidean space, such poles can be purely imaginary (as in the NJL model which only has one pole of this type) or fully complex. The existence of these poles implies the appearance of "pinch points" [16] in the calculation of the meson two-point functions. The

external momentum for which the first of such "pinch points" appears is given by $p_{pp} = 2S_i$ where S_i is the imaginary part of the first pole of the quark propagator. From this point on the functions G in Eq.(17) do in general develop an imaginary component related to the unphysical decay into $q\bar{q}$ pairs, which is usually associated with the lack of confinement. In some cases, depending on the regulator and/or parametrization, one can find a prescription for the integration path along the complex plane such that this imaginary component cancels out[16, 17, 34]. It is clear, however, that the corresponding results turn out to be prescription dependent and, unless the meson pole appears no far above p_{pp}, not very reliable. For this reason, in this work we take the point of view that p_{pp} marks the limit of validity of our model. For the three scenarios under consideration we have found p_{pp} to be about 1 GeV, which appears to be a reasonable scale for a low energy effective model of QCD. As for the σ' channel we have verified that no pole corresponding to a meson of this type appears below that scale.

We turn now to the low-energy parameters for $\pi - \pi$ scattering. These parameters have been matter of much attention in the recent past years. In particular, recent results on Kl4 decays [35, 36] have led to an improved phenomenological determination[37, 38] of the threshold parameters for S-, P-, D- and F- waves. Our results for the S and P waves are displayed in Table II while those corresponding to D and F waves in Table III. Since the calculation of sigma pole contributions include off-shell quantities it is not possible to perform a clear and unique separation between σ and σ' contributions. Thus, only the sum of such contributions is given. In general, reasonable estimates indicate that σ' contributions represent only a few percent of this total value. The phenomenological values extracted in Ref.[38] are also indicated. In comparing our results with these values one should keep in mind that the present model does not incorporate pion loops, and hence there is still room for improvement. Finally, for comparison, in Tables II and III the existing results for the local SU(2) NJL model [39, 40] are given. Results obtained in alternative QCD-based quark models can be found, e.g. in Ref.[41]

We analyze first the results corresponding to the S- and P-waves. Let us recall that to leading order in the chiral expansion the corresponding length and slope parameters can be obtained from the Weinberg amplitude

$$A\left(s,t,u\right) = \frac{s - f_\pi^2}{m_\pi^2} \tag{56}$$

which leads to the predictions

$$\frac{8}{7}\, a_0^0 \cdot m_\pi = -4\; a_0^2 \cdot m_\pi = b_0^0 \cdot m_\pi^3 = -2\; b_0^2 \cdot m_\pi^3 = 6\; a_1^1 \cdot m_\pi^3 = \frac{m_\pi^2}{4\;\pi\;f_\pi^2} \tag{57}$$

Since our three different scenarios lead to the same values of f_π and m_π the predictions for these five scattering parameters are expected to be quite similar. In fact, results in Table II confirm this, although those of S2 are in slightly better agreement with empirical data. This is particularly interesting in the case of a_0^2, which results from a rather strong cancellation between box and sigma contributions. In order to be more sensitive in the comparison between scenarios, we also give in Table II the combination of the S-wave isospin 0 and 2 parameters $2a_0^0 + 7a_0^2$ which vanishes in the chiral limit. We observe that in all scenarios the correction goes in the right direction. Moreover, in the case of S2 its magnitude is larger providing therefore a better description of the experimental result. Another way to improve on the discrimination between the different parametrizations of our model is to consider corrections up to q^6 order in the expansion Eq.(46). Thus, we calculate the parameters c_l^I and d_l^I corresponding to the q^4 and q^6 corrections, respectively. We observe that in each partial wave the exponential interaction produces scattering parameters which decrease rather fast with the power of q^2. On the other hand, the scenario S2 predicts coefficients which are of the same order of magnitude in each partial wave.

We consider now the scattering lengths and slope parameters for D- and F-waves displayed in Table III. These results, together with the scattering lengths and slope parameters of S- and P-waves given in Table II, complete all cases for which there are phenomenological determinations available. For S1 and S3, we observe that the signs of the parameters are correctly predicted, except for b_2^0 in S3. The absolute values for the scattering lengths are off by a factor between 1.5 and 2.5, whereas the slope parameters fail by one order of magnitude. On the other hand, the scenario S2 gives the right sign and order of magnitude in all cases, deviating only by a factor 3 in the worse case, b_3^1.

From the previous results we can conclude that although the exponential interaction might be able to reproduce the scattering lengths parameters rather well the description of higher power coefficients is, in general, expected to be less accurate as the power in q^2 increases. This is particularly so for the higher partial waves. On the other hand, the momentum dependence of the scenario S2 seems to be better adapted for the description of the higher power parameters. In fact, the only case where this scenario gives a worse result than the exponential ones is in the prediction for b_1^1, where a strong cancellation between the box and sigma contribution takes place.

Comparing scenarios S1 and S3 we can observe the effect on the scattering parameters of taking into account the wave function renormalization. Except for the parameters listed in Eq.(57), we observe that as the power in q^2 increases the associated parameters obtained in scenario S3 decrease faster than in scenario S1. We can conclude that

the effect of the wave function renormalization term goes in the right direction, even if this effect is less important than the one produced by the difference in the momentum dependence of the interactions. It should be noticed that our scenario S3 is very similar to the model used in Ref.[42]. In fact, in both cases the wave function renormalization is not included, exponential parameterizations are used and the values of m_π and f_π are fitted. The difference comes from the way in which the third parameter of the model is determined. In Ref.[42] the rather sensitive value of a_2^2 was used, while here we choose to fix the chiral condensate.

In our scenarios which include wavefunction renormalization we have fixed $Z(0) = 0.7$. As it can be seen in Fig.1, however, for small values of p the errors in the lattice results are rather large. Thus, $Z(0)$ is not well constrained by lattice calculations. In order to test the sensitivity of our results to this kind of uncertainties we have reduced it to $Z(0) = 0.6$, and considered the scenario S2 for two alternative situations. In the first case we varied the model parameters so that f_π and m_π remain at their empirical values, while in the second case we kept the model parameters fixed. In both cases we found that most of our results change by less that 10%, the most notorious exception being the $\pi\pi$ scattering length a_2^2 which changes about 15 %. It is interesting to note that in the second case the pion mass and decay constant, as well as the chiral condensate, get reduced. We obtain $m_\pi = 138.7\ MeV$, $f_\pi = 91.2\ MeV$ and $-<\bar{q}q>^{1/3}= 323\ MeV$.

V. COMPARISON WITH CHIRAL PERTURBATION THEORY

In the previous section we have focused our attention on the ability of our quark model to reproduce the phenomenological π-π scattering parameters. An alternative point of view (see, for example Refs. [39, 43, 44, 45, 46, 47]) is to consider the quark models as the generators of the pion Chiral Perturbation Theory (χPT) Lagrangian[21]. χPT describes the low energy physics of pions in a universal way, once the order in the momentum and chiral breaking expansion (i.e. the order in the chiral expansion) is specified. Different scenarios for quark models will lead to χPT Lagrangians with different values of the so-called low energy constants (LECs). In this section we analyze the connection between our quark scenarios and the χPT Lagrangian up to the fourth order in the chiral expansion.

To perform this connection we introduce the pionic Lagrangian

$$\mathcal{L} = \mathcal{L}_2 + \mathcal{L}_4 \ , \tag{58}$$

where

$$\mathcal{L}_2 = \frac{f^2}{4}\left\langle \partial_\mu U^\dagger\ \partial^\mu U + U^\dagger\chi + \chi^\dagger U\right\rangle \qquad , \tag{59}$$

$$\mathcal{L}_4 = \ell_1\left\langle \partial_\mu U^\dagger\ \partial^\mu U\right\rangle^2 + \ell_2\left\langle \partial_\mu U^\dagger\ \partial_\nu U\right\rangle\left\langle \partial^\mu U^\dagger\ \partial^\nu U\right\rangle^2 + \ell_3\left\langle \chi U\right\rangle^2 + \ell_4\left\langle \partial_\mu\chi\ \partial^\mu U\right\rangle^2 + ... \quad , \tag{60}$$

and

$$U = \exp\left(i\frac{\vec{\tau}.\vec{\pi}}{f}\right) \qquad ; \qquad \chi = m^2\begin{pmatrix} 1 & 0 \\ 0 & 1\end{pmatrix} \quad . \tag{61}$$

Note that among all possible $O(4)$ terms only those relevant for π-π scattering to that order have been explicitly given. To the order we are working, the parameters f and m can be related with the predicted values for f_π and m_π through

$$f_\pi = f\left(1 + \left(\frac{m_\pi}{f_\pi}\right)^2\ell_4\right) \ , \tag{62}$$

$$m_\pi^2 = m^2\left(1 + 2\left(\frac{m_\pi}{f_\pi}\right)^2\ell_3\right) \ . \tag{63}$$

Using (62) and (63), we can express the scattering parameters resulting from Eq.(58) in terms of the ℓ_i coupling

constants and the m_π and f_π values as follows

$$
\begin{aligned}
m_\pi\ a_0^0 &= \frac{7}{32\pi}\left(\frac{m_\pi}{f_\pi}\right)^2\left\{1+\frac{1}{7}\left(\frac{m_\pi}{f_\pi}\right)^2[40\ \ell_1+40\ \ell_2+10\ \ell_3+14\ \ell_4]\right\}\\
m_\pi\ a_0^2 &= -\frac{1}{16\pi}\left(\frac{m_\pi}{f_\pi}\right)^2\left\{1-\left(\frac{m_\pi}{f_\pi}\right)^2[8\ \ell_1+8\ \ell_2+2\ \ell_3-2\ \ell_4]\right\}\\
m_\pi^3\ b_0^0 &= \frac{1}{4\pi}\left(\frac{m_\pi}{f_\pi}\right)^2\left\{1+\frac{1}{4}\left(\frac{m_\pi}{f_\pi}\right)^2[64\ \ell_1+48\ \ell_2+8\ \ell_4]\right\}\\
m_\pi^3\ b_0^2 &= -\frac{1}{8\pi}\left(\frac{m_\pi}{f_\pi}\right)^2\left\{1-\frac{1}{2}\left(\frac{m_\pi}{f_\pi}\right)^2[16\ \ell_1+24\ \ell_2-4\ \ell_4]\right\}\\
m_\pi^3\ a_1^1 &= \frac{1}{24\pi}\left(\frac{m_\pi}{f_\pi}\right)^2\left\{1+\left(\frac{m_\pi}{f_\pi}\right)^2[-8\ \ell_1+4\ \ell_2+2\ \ell_4]\right\}\\
m_\pi^5\ b_1^1 &= \frac{1}{6\pi}\left(\frac{m_\pi}{f_\pi}\right)^4\{-2\ \ell_1+\ell_2\}\\
m_\pi^5\ a_2^0 &= \frac{1}{15\pi}\left(\frac{m_\pi}{f_\pi}\right)^4\{\ell_1+2\ \ell_2\}\\
m_\pi^5\ a_2^2 &= \frac{1}{30\pi}\left(\frac{m_\pi}{f_\pi}\right)^4\{2\ \ell_1+\ell_2\}
\end{aligned}
\tag{64}
$$

As already mentioned, the Lagrangian (58) is valid up to fourth order in the chiral expansion, therefore it can be fully equivalent to our quark model scenarios only when they are treated to the same order of approximation. Thus, to extract the LECs defining the pionic Lagrangian from the values of the scattering parameters, f_π and m_π obtained in each of our quark scenarios we should analyze the values of these parameters for small values of m_c. In fact, we have verified that close to the chiral limit the scattering parameters display, as a function of $(m_\pi/f_\pi)^2$, the quadratic behavior expected from Eqs.(64). From the determination of the corresponding linear and quadratic coefficients it is possible to obtain the numerical values of LECs ℓ_i. It should be noticed that this procedure for obtaining ℓ_i is completely equivalent to the bosonization of the quark Lagrangian followed by a covariant gradient expansion (see Ref.[39] for the application of such method to the NJL model). At this stage we are connecting our quark model at the one loop level to the pionic Lagrangian at the tree level. Our next step is to make the connection with the χPT Lagrangian. The main difference between the Lagrangian (58) and the χPT Lagrangian is that our ℓ_i parameters are finite and no pion loop contribution is present. The scattering parameters in χPT [21] include pion loop contributions, and are written in terms of renormalized LECs ℓ_i^r. As expected, Eqs.(64) coincide with the ones obtained from χPT if the corresponding pion loop contributions are neglected. In this approximation the coupling constants ℓ_i can be identified with the ℓ_i^r constants at some given renormalization scale μ.

Eqs.(64) imply several relations between the scattering parameters. We focus on two of them

$$
Test1 = m_\pi\ \left(2\ a_0^0-5\ a_0^2\right)+m_\pi^3\ \left(-\frac{9}{2}a_1^1-b_0^0+\frac{5}{2}b_0^2\right)=\left\{\begin{array}{cc} 0 & \text{using (64)}\\ \frac{m_\pi^4}{16\pi^4 f_\pi^4}\frac{17\pi}{12} & \text{using } \chi\text{PT}\end{array}\right. \tag{65}
$$

$$
Test2 = \frac{5}{2}\ m_\pi\ a_2^2+\frac{3}{10}\ m_\pi\ b_1^1-m_\pi\ a_2^0=\left\{\begin{array}{cc} 0 & \text{using (64)}\\ \frac{1}{16\pi^4 f_\pi^4}\frac{7\pi}{450} & \text{using } \chi\text{PT}\end{array}\right. \tag{66}
$$

Obviously these two relations vanish when we use our pionic Lagrangian (58) at the tree level. Therefore, a non-vanishing value obtained for these two quantities in any other calculation must be originated by loop corrections or by higher order terms in the chiral expansion. As indicated in Eqs.(65,66), in the case of the χPT Lagrangian both relations have corrections from pionic loops. On the other hand, the deviation from zero of $Test1$ and $Test2$ when evaluated using the scattering parameters obtained in our quark scenarios at the physical value of m_π is originated by higher order terms in the chiral expansion. In Table IV we show the results for these two relations in our scenarios. Also indicated are the χPT Lagrangian results, which corresponds to the pion loop contribution of the order $(m_\pi/2\pi f_\pi)^4$. From this table we observe that the quark scenarios previously studied give results for $Test1$ and $Test2$ which are of the same order of magnitude than the pion loop contributions. This implies that the studied quark models include

higher order contributions (i.e. O(6) or higher) which are as important as the chiral loops. The effect of these higher order contributions is more important for the scenario S2, due to its different behavior for large momenta.

In Table V we give the ℓ_i values corresponding to our different scenarios. It is interesting to note that in the case of ℓ_1 the listed values result, in all cases, from an important cancellation between the box and the sigma contributions. For ℓ_2 only box contribution is present since no scalar meson contribution is possible [48]. Also given in Table V are the values of the renormalized LECs $\ell_i^r(\mu)$ obtained[37] in the framework of χPT at some particular values of renormalization scale μ[49]. We observe that the sign and order of magnitude of the most accurately known LECs ℓ_2^r and ℓ_4^r are well reproduced for small values of μ. In fact, in the case of the scenarios S1 and S2 the agreement is remarkable good for μ around 2 m_π which is a reasonable scale since we have integrated out degrees of freedom from below the sigma mass. In the case of the LECs ℓ_1^r and ℓ_3^r, even though it is not so good in the case of S2, the agreement is still acceptable given the existing uncertainties in the determination of the empirical values. Finally, as a reference, some typical values obtained within the local NJL model taken from Ref.[39] are also listed in Table V.

VI. CONCLUSIONS

In this work we have analyzed the sigma meson mass and width together with the π-π scattering parameters in the context of non-local chiral quark models with wave-function renormalization (WFR) term. We have considered two types of momentum dependence for the quark interactions. The first one (scenario S1) is based on the frequently used exponential form factors. The second one (scenario S2) corresponds to a fit to the mass and renormalization functions obtained in lattice calculations[8], and gives rise to a softer momentum dependence (e.g. at large momentum, the quark mass decreases as $(p^2)^{-3/2}$ instead of exponentially). In order to test the influence of the WFR, we also considered a third scenario S3 which corresponds to an exponential interaction but where this renormalization is absent.

Our results for the sigma mass are relatively stable, ranging from 552 MeV for S2 to 683 MeV for S3. We observe that the coupling between the scalar term of the standard chiral interaction and the new scalar term associated with the WFR term reduces the value of the lower sigma mass, as it must be expected. Comparing the S3 and S1 results we observe a reduction of a 10%, while in the case of the S2 interaction there is a further reduction of 10% originated by the softer momentum dependence of the interaction. The width of the sigma follows the same reduction as its mass, as one goes from one scenario to another. These results are less dependent on the parameterization than in the standard NJL model. The predicted mass and width are reasonable close to the recently reported empirical values [32, 33].

Regarding the $\pi - \pi$ scattering parameters, we have compared our results with the phenomenological determination made in Ref.[38]. Although the existence of the chiral limit relations, Eqs.(57), for the S- and P-wave scattering length and slope parameters reduces the sensitivity of these parameters to the choice of the different quark interactions, we have been able to discriminate between these interactions by going to higher order in the momentum expansion or to higher partial waves. We conclude that although the exponential interaction is able to reproduce the scattering lengths parameters rather well the description of higher power coefficients turns out to be, in general, less accurate as the power in q^2 increases. This can be clearly seen in the case of higher partial waves. On the other hand, the momentum dependence of the scenario S2 seems to be better adapted for the description of the existing empirical data. Comparing the predictions of the scenarios based on exponential interactions, S1 and S3, we observe that the presence of the WFR term tends to improve the results, even though its effect is less noticeable that the one produced by the difference on the momentum dependence of the interactions.

Finally, we have analyzed the relation of our quark scenarios with the chiral Lagrangian up to $O(4)$ in the chiral expansion. In particular, we have obtained predictions for the low energy constants ℓ_i involved in π-π scattering within our scenarios. The procedure we followed, using the scattering parameters, is equivalent to the standard method of bosonization followed by covariant gradient expansion. Our predicted values for ℓ_i are in relative good agreement with the values for the renormalized ℓ_i^r constants defined in the χPT calculations [21] for a μ value about $2m_\pi$. They are also in the range of values obtained in the NJL model calculation of Ref. [39]. We have been able to define combinations of the scattering parameters which allow to discriminate between higher chiral corrections (O(6) or higher) and pion loop corrections. We observe that the higher order corrections included in our non-local quark model calculations at physical m_π are of the same order that the pion loop corrections not considered in this work. The effect of such corrections in our predictions for the mesonic observables is an issue that deserves further investigation.

Acknowledgements

The authors wish to thank D. Gomez Dumm and J. Portoles for useful discussions. NNS acknowledges the support of CONICET (Argentina) grant PIP 6084, and ANPCyT (Argentina) grant PICT04 03-25374, and SN the support of the Sixth Framework Program of the European Commision under the Contract No. 506078 (I3 Hadron Physics) and MEC (Spain) under the Contract FPA 2007-65748-C02-01 and EU FEDER.

---

[1] Y. Nambu and G. Jona-Lasinio, Phys. Rev. **122**, 345 (1961); Phys. Rev. **124**, 246 (1961).
[2] U. Vogl and W. Weise, Prog. Part. Nucl. Phys. **27**, 195 (1991).
[3] S. P. Klevansky, Rev. Mod. Phys. **64**, 649 (1992).
[4] T. Hatsuda and T. Kunihiro, Phys. Rept. **247**, 221 (1994).
[5] G. Ripka, *Quarks bound by chiral fields* (Oxford University Press, Oxford, 1997).
[6] T. Schafer and E. V. Shuryak, Rev. Mod. Phys. **70**, 323 (1998).
[7] C. D. Roberts and A. G. Williams, Prog. Part. Nucl. Phys. **33**, 477 (1994); C. D. Roberts and S. M. Schmidt, Prog. Part. Nucl. Phys. **45**, S1 (2000).
[8] M. B. Parappilly, P. O. Bowman, U. M. Heller, D. B. Leinweber, A. G. Williams and J. B. Zhang, Phys. Rev. D **73**, 054504 (2006).
[9] P. O. Bowman, U. M. Heller, D. B. Leinweber and A. G. Williams, Nucl. Phys. Proc. Suppl. **119** (2003) 323. P. O. Bowman, U. M. Heller, and A. G. Williams, Phys. Rev. D **66** (2002) 014505.
[10] S. Furui and H. Nakajima, Phys. Rev. D **73**, 074503 (2006).
[11] E. Ruiz Arriola and L. L. Salcedo, Phys. Lett. B **450**, 225 (1999).
[12] D. Blaschke, Y. L. Kalinovsky, G. Roepke, S. M. Schmidt and M. K. Volkov, Phys. Rev. C **53**, 2394 (1996).
[13] G. Ripka, Nucl. Phys. A **683**, 463 (2001); R. S. Plant and M. C. Birse, Nucl. Phys. A **703**, 717 (2002).
[14] S. Noguera, Int. J. Mod. Phys. E **16**, 97 (2007).
[15] S. Noguera and V. Vento, Eur. Phys. J. A **28**, 227 (2006).
[16] R. D. Bowler and M. C. Birse, Nucl. Phys. A **582**, 655 (1995). R. S. Plant and M. C. Birse, Nucl. Phys. A **628**, 607 (1998).
[17] A. Scarpettini, D. Gomez Dumm and N. N. Scoccola, Phys. Rev. D **69**, 114018 (2004).
[18] D. Gomez Dumm, A. G. Grunfeld and N. N. Scoccola, Phys. Rev. D **74**, 054026 (2006).
[19] B. Golli, W. Broniowski and G. Ripka, Phys. Lett. B **437**, 24 (1998); W. Broniowski, B. Golli and G. Ripka, Nucl. Phys. A **703**, 667 (2002).
[20] A. H. Rezaeian, N. R. Walet and M. C. Birse, Phys. Rev. C **70**, 065203 (2004); A. H. Rezaeian and H. J. Pirner, Nucl. Phys. A **769**, 35 (2006).
[21] J. Gasser and H. Leutwyler, Annals Phys. **158**, 142 (1984); J. Gasser and H. Leutwyler, Nucl. Phys. B **250**, 465 (1985).
[22] E. Ruiz Arriola and W. Broniowski, Phys. Rev. D **67** (2003) 074021 [arXiv:hep-ph/0301202].
[23] H. G. Dosch and S. Narison, Phys. Lett. B **417**, 173 (1998).
[24] L. Giusti, F. Rapuano, M. Talevi and A. Vladikas, Nucl. Phys. B **538**, 249 (1999).
[25] G. Colangelo, J. Gasser and H. Leutwyler, Phys. Rev. Lett. **86**, 5008 (2001).
[26] W. M. Yao *et al.* [Particle Data Group], J. Phys. G **33**, 1 (2006).
[27] M. Jamin, Phys. Lett. B **538**, 71 (2002).
[28] V. Gimenez, V. Lubicz, F. Mescia, V. Porretti and J. Reyes, PoS **LAT2005**, 081 (2006).
[29] V. Gimenez, V. Lubicz, F. Mescia, V. Porretti and J. Reyes, Eur. Phys. J. C **41**, 535 (2005).
[30] D. Becirevic *et al.*, PoS **LAT2005**, 079 (2006).
[31] K. Nakayama and S. Krewald, Phys. Lett. B **273**, 199 (1991).
[32] E. M. Aitala *et al.* [E791 Collaboration], Phys. Rev. Lett. **86**, 770 (2001).
[33] N. Wu, arXiv:hep-ex/0104050.
[34] M. Praszalowicz and A. Rostworowski, Phys. Rev. D **64**, 074003 (2001) [arXiv:hep-ph/0105188].
[35] S. Pislak *et al.* [BNL-E865 Collaboration], Phys. Rev. Lett. **87**, 221801 (2001).
[36] A. Aloisio *et al.* [KLOE Collaboration], Phys. Lett. B **538**, 21 (2002).
[37] G. Colangelo, J. Gasser and H. Leutwyler, Nucl. Phys. B **603**, 125 (2001).
[38] R. Kaminski, J. R. Pelaez and F. J. Yndurain, arXiv:0710.1150 [hep-ph].
[39] C. Schuren, E. Ruiz Arriola and K. Goeke, Nucl. Phys. A **547**, 612 (1992).
[40] V. Bernard, A. A. Osipov and U. G. Meissner, Phys. Lett. B **285**, 119 (1992).
[41] C. D. Roberts, R. T. Cahill, M. E. Sevior and N. Iannella, Phys. Rev. D **49** (1994) 125; P. Bicudo, Phys. Rev. C **67**, 035201 (2003); S. R. Cotanch and P. Maris, Phys. Rev. D **66**, 116010 (2002); P. Bicudo, S. Cotanch, F. J. Llanes-Estrada, P. Maris, E. Ribeiro and A. Szczepaniak, Phys. Rev. D **65**, 076008 (2002).
[42] A. A. Osipov, A. E. Radzhabov and M. K. Volkov, arXiv:hep-ph/0603130.
[43] B. Holdom, J. Terning and K. Verbeek, Phys. Lett. B **232**, 351 (1989); B. Holdom, J. Terning and K. Verbeek, Phys. Lett. B **245**, 612 (1990) [ERRATUM.ibid.B273:549,1991]; B. Holdom, Phys. Rev. D **45**, 2534 (1992).
[44] M. R. Frank and T. Meissner, Phys. Rev. C **53** (1996) 2410.
[45] H. Yang, Q. Wang and Q. Lu, Phys. Lett. B **532**, 240 (2002); H. Yang, Q. Wang, Y. P. Kuang and Q. Lu, Phys. Rev. D

66, 014019 (2002).
[46] F. J. Llanes-Estrada and P. De A. Bicudo, Phys. Rev. D **68**, 094014 (2003).
[47] H. A. Choi and H. C. Kim, Phys. Rev. D **69**, 054004 (2004).
[48] G. Ecker, J. Gasser, A. Pich and E. de Rafael, Nucl. Phys. B **321,** (1989) 311.
[49] It should be noticed that f_π and m_π are also affected by the pion loops. For $\mu = 2m_\pi$ the pion loops produce a factor 1.02 for f_π and a factor 0.99 for m_π^2. This effect has been neglected in the present discussion.

Table I: Model parameters and results for some alternative parameterizations.

		S1	S2	S3
m_c	MeV	5.70	2.37	5.78
$G_s\Lambda_0^2$		32.03	20.82	20.65
Λ_0	MeV	814.42	850.00	752.2
$\varkappa_P$	GeV	4.18	6.03	–
Λ_1	MeV	1034.5	1400	–
$\bar{\sigma}_1$	MeV	529	442	424
$\bar{\sigma}_2$		-0.43	-0.43	–
$M(0)$	MeV	375	311	430
$Z(0)$		0.7	0.7	1.0
$-<q\bar{q}>^{1/3}$	MeV	240	326	240
m_π	MeV	139	139	139
$g_{\pi q\bar{q}}$		5.74	4.74	4.62
f_π	MeV	92.4	92.4	92.4
m_σ	MeV	622	552	683
$g^{(0)}_{\sigma q\bar{q}}$		5.97	4.60	5.08
$g^{(1)}_{\sigma q\bar{q}}$		-0.77	-0.26	–
$\Gamma_{\sigma\pi\pi}$	MeV	263	182	347

Table II: $\pi - \pi$ scattering parameters for S and P waves.

	contribution	S1	S2	S3	NJL		Empirical
					Ref.[39]	Ref.[40]	Ref.[38]
$(m_\pi) \times a_0^0$	box	-1.536	-1.279	-1.618			
	σ	1.718	1.470	1.798			
	Total	0.182	0.191	0.180	0.18	0.19	0.223 ± 0.009
$(m_\pi^3) \times b_0^0$	box	0.114	0.117	0.114			
	σ	0.116	0.146	0.107			
	Total	0.230	0.263	0.221	0.22	0.27	0.290 ± 0.006
$(m_\pi^5) \times c_0^0$	box	-0.0086	0.0233	-0.0076			
	σ	0.0412	0.0663	0.0302			
	Total	0.0326	0.0897	0.0226			
$(m_\pi^7) \times d_0^0$	box	0.0005	0.065	0.0004			
	σ	0.0087	0.019	0.0051			
	Total	0.0092	0.085	0.0055			
$(m_\pi) \times a_0^2$	box	-0.6851	-0.5790	-0.7170			
	σ	0.6404	0.5346	0.6721			
	Total	-0.0447	-0.0444	-0.0449	-0.046	-0.044	-0.0444 ± 0.0045
$(m_\pi^3) \times b_0^2$	box	-0.053	-0.049	-0.051			
	σ	-0.031	-0.034	-0.033			
	Total	-0.084	-0.083	-0.084	-0.091	-0.079	-0.081 ± 0.003
$(m_\pi^5) \times c_0^2$	box	0.0080	0.0078	0.0082			
	σ	0.0042	0.0056	0.0034			
	Total	0.0121	0.0134	0.0116			
$(m_\pi^7) \times d_0^2$	box	-0.0005	-0.0006	-0.0005			
	σ	-0.0006	-0.0011	-0.0004			
	Total	-0.0011	-0.0017	-0.0009			
$m_\pi \times (2a_0^0 + 7a_0^2)$		0.052	0.072	0.046	0.04	0.072	0.135 ± 0.036
$(m_\pi^3\ 10^3) \times a_1^1$	box	25.1	23.9	24.7			
	σ	10.5	11.3	11.1			
	Total	35.7	35.2	35.7	37	34	38.1 ± 0.9
$(m_\pi^5\ 10^3) \times b_1^1$	box	5.56	4.60	5.34			
	σ	-2.10	-2.85	-1.72			
	Total	3.45	1.75	3.62			5.13 ± 0.15
$(m_\pi^7\ 10^3) \times c_1^1$	box	0.21	-2.70	0.15			
	σ	0.38	0.63	0.25			
	Total	0.59	-2.06	0.40			

Table III: Scattering lengths and slope parameters for D and F waves.

	contribution	S1	S2	S3	NJL Ref.[39]	NJL Ref.[40]	Empirical Ref.[38]
$(m_\pi^5\ 10^4)\times a_2^0$	box	9.71	9.76	9.93			
	σ	4.20	5.67	3.44			
	Total	13.91	15.43	13.37	13.7	16.7	18.33 ± 0.36
$(m_\pi^7\ 10^4)\times b_2^0$	box	0.98	0.85	1.04			
	σ	-1.28	-2.20	-0.86			
	Total	-0.30	-1.34	0.18			-3.82 ± 0.25
$(m_\pi^5\ 10^4)\times a_2^2$	box	-2.74	-2.95	-2.43			
	σ	4.20	5.67	3.44			
	Total	1.46	2.72	1.01	1.1	3.2	2.46 ± 0.25
$(m_\pi^7\ 10^4)\times b_2^2$	box	0.08	0.07	0.13			
	σ	-1.28	-2.20	-0.86			
	Total	-1.19	-2.14	-0.73			-3.59 ± 0.18
$(m_\pi^7\ 10^5)\times a_3^1$	box	0.82	1.15	0.7			
	σ	1.82	3.09	1.2			
	Total	2.65	4.24	1.9			6.05 ± 0.29
$(m_\pi^9\ 10^5)\times b_3^1$	box	0.06	0.0	0.07			
	σ	-0.70	-1.6	-0.40			
	Total	-0.64	-1.6	-0.33			-4.41 ± 0.36

Table IV: Results for $Test1$ and $Test2$ defined in Eqs.(65,66) as obtained in our quark scenarios (S1,S2 and S3) and Chiral Perturbation Theory to O(4) (χPT). The results obtained using the empirical values of Ref.[38] (Empirical) are also given.

	S1	S2	S3	χPT	Empirical [38]
$Test1\times10^2$	-1.2	-2.5	-1.1	1.5	0.40 ± 4.4
$Test2\times\left(m_\pi^4\ 10^4\right)$	0.1	-3.3	0.006	1.6	3.21 ± 1.4

Table V: Values of ℓ_i obtained in our different scenarios. The χPT values of ℓ_i^r as a funtion of μ are obtained from Ref.[37]. The last two columns corresponds to the NJL predictions from Ref. [39] for two different constituent quark mass: $M=220$,264 MeV.

	Non Local Quark Model			χPT ($\ell_i^r(\mu)$)			NJL	
	S1	S2	S3	$\mu=m_\rho$	$\mu=2\ m_\pi$	$\mu=m_\pi$	$M=220$	$M=264$
$\ell_1\times10^3$	-1.39	0.26	-2.07	-4.0 ± 0.6	-1.9 ± 0.6	-0.4 ± 0.6	-0.63	-2.28
$\ell_2\times10^3$	6.46	6.41	6.51	1.9 ± 0.2	6.2 ± 0.2	9.1 ± 0.2	6.29	6.18
$\ell_3\times10^3$	-2.3	-4.1	-1.1	1.5 ± 4.0	-1.8 ± 4.0	-4.0 ± 4.0	-8.50	-3.48
$\ell_4\times10^3$	17.2	20.3	15.0	6.2 ± 1.3	19.1 ± 1.3	27.9 ± 1.3	22.73	12.16

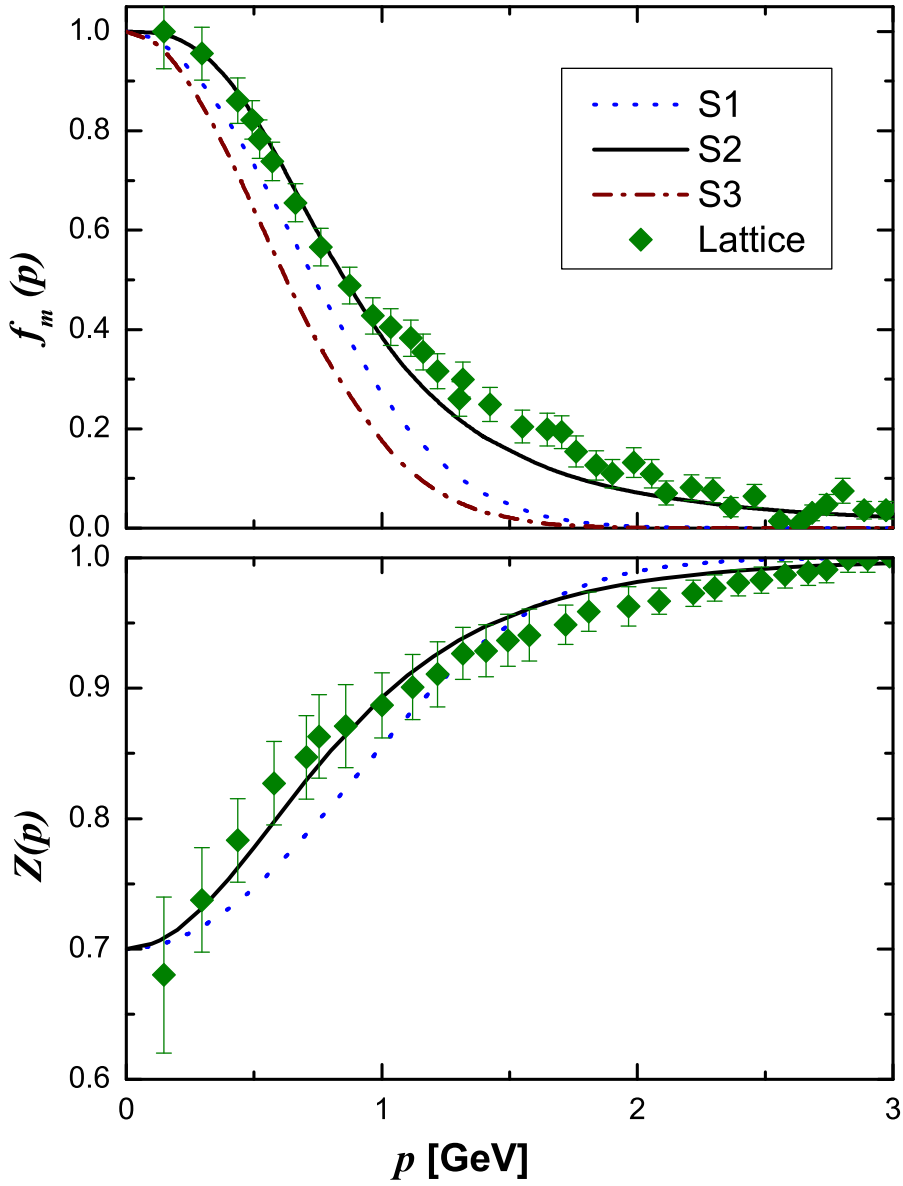

Figure 1: (Color online) $f_m(p)$ (Upper panel) and $Z(p)$ (lower panel) for various parametrization as compared with Lattice results of Ref. [8]